УДК 621.396.677

M.M. Dergousov, I.N. Trofimov, V.O. Tutunnik, A.F. Shevchenko

Kharkov University Air Force named after Ivan Kozhedub, Kharkov

COMPARATIVE DIRECTIONAL CHARACTERISTICS ANALYSIS OF CIRCULAR PHASED ARRAYS FOR CONSTRUCTING ACTIVE AND PASSIVE MULTISTATIC RADARS

Brought results numerical dependences analysis of circular phased array directional characteristics created from elementary electric feed elements for different types of amplitude-phased distributions and data points in design parameters of antenna system. The results can be used for selecting antenna type of active and passive multistatic systems designed for establishing entire radar field.

Keywords: *multistatic radar, circular phased array, directional characteristics.*

General task statement

Actual question of airspace control is establishing and maintaining entire original airspace in low-level heights. Absence of reliable radar control in low-level heights makes precondition its illegal using. In particular there is increasing level of dangerous threat of terrorism from air during flight in quantities of aviation in this flights. As shown in [1] establishing low-level flights of radar field it is reasonable to create active and passive multistatic radars with electronic scanning on the basis of circular phased arrays (CPA) L-range situated on the towers. Such an approach provides high rate of unification received and transmitted apparatus of each position and allow:

– detect air targets in active mode for account of active radars with CPA in the capacity of multistatic positions;

– increase accuracy of estimating azimuth of targets in active mode for account of range methods in estimating without increasing size of antennas;

– detect targets in passive multistatic mode (in the field of illumination of cellular communications stations, by means of irradiating board installation in secondary radar systems RBS, MK-XA(XII), Password);

– create frequency bands for satellite navigators of air objects, in particular unmanned aerial vehicles (UAV) and so on.

The example of unification using automatic radar with CPA in L-range on the towers is shown on the fig. 1.

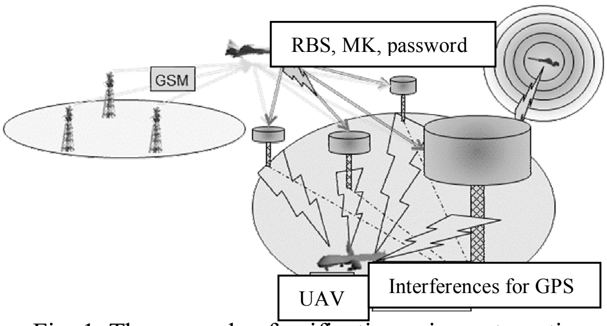

Fig. 1. The example of unification using automatic radar on the towers with CPA in L-range

It should be noted that using CPA or another arrays with axial symmetry one can achieve in multistatic radar such advantages:

– reduced-order control of air surveillance modes in comparison with mechanical antennas rotation for account of possible orientation main maximum of CPA pattern in azimuth direction with high speed;

– widening active zone of multistatic radar for account of absence directivity variation of CPA by azimuth in comparison with plane and linear arrays;

– possibilities of work in wide frequency band with constant directivities for account of huge range and broadbandness of axial arrays in comparison with plane and another ones.

It is conditional on actuality of aim article in analysis of CPA directional characteristics (DC) dependences on their design factors and types of amplitude-phase distribution (APD) in constructing multistatic radar for creating low-level height radar field. For analysis it is chosen method of computational modeling of axial-symmetric arrays shown in [2]. Method allows getting upper bounds of CPA DC of resonance length dipole radiator in different variants of constructive fulfilling array and using measures for decreasing interference of radiators.

1. Mathematical model of CPA

One consider CPA created from elementary non-commuted electric dipoles in free space fig. 2. Electric and magnetic component in far-field region in what the dipole is allocating in point $\vec{X}_n$ if $\left|\vec{X}-\vec{X}_n\right| >> \lambda_0$ designate as [2]:

$$\dot{\vec{E}}_n\left(\vec{X}\middle|\vec{X}_n, \dot{I}_n\right) = \frac{\dot{I}_n k_0}{j4\pi R_n}\sqrt{\frac{\mu_0}{\varepsilon_0}}\vec{s}_n^{\,T} \cdot e^{jk_0\left(\vec{R}_n^{\,0}\vec{X}+R_n\right)}, \quad (1)$$

$$\dot{\vec{H}}_n\left(\vec{X}\middle|\vec{X}_n, \dot{I}_n\right) = -\frac{\dot{I}_n k_0}{j4\pi R_n}\vec{s}_n^{\,\perp} \cdot e^{jk_0\left(\vec{R}_n^{\,0}\vec{X}+R_n\right)}, \quad (2)$$

where $\vec{X}$ – radius of point vector observation, in far-field region; $\vec{X}_n$ – radius vector of allocating dipole; $\dot{I}_n$ – complex amplitude of dipole current; $k_0 = \omega_0\sqrt{\mu_0\varepsilon_0}$ – wave number of circular frequency $\omega_0 = 2\pi c/\lambda_0$; ε_0, μ_0 – electric and magnetic permeability; $R_n = \left|\vec{X}-\vec{X}_n\right|$ – distance from n-dipole to observation point (OP); $\vec{s}_n^{\,T} = \vec{s}_n - \vec{R}_n^{\,0} \cdot \left(\vec{R}_n^{\,0} \cdot \vec{s}_n\right)$, $\vec{s}_n^{\,\perp} = \vec{R}_n^{\,0} \times \vec{s}_n$ – vector components $\vec{s}_n$, which take into consideration orientation and dipole length $\left|d\vec{l}\right|$ with vector-moment $\dot{\vec{p}}_n = \dot{I}_n \left(j\omega_0\right)^{-1} d\vec{l}$.

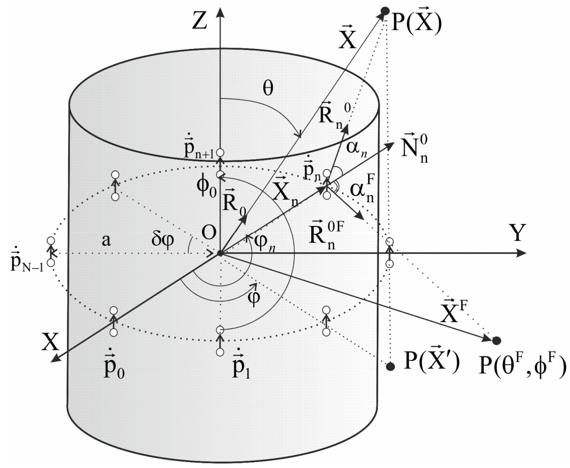

Fig. 2. Geometrical model of CPA

One propose that CPA radiators are ideally coordinated with power feeder then current dipole amplitude are designated [3]:

$$\dot{I}_n = \frac{\left|d\vec{l}\right|}{\pi\lambda_0}\sqrt{\frac{P_n}{80}}, \quad (3)$$

where P_n – brought power.

From expressions (1), (2) there is following result. If OP is designated as radius vector:

$$\vec{X}^F = \left|\vec{X}^F\right| \cdot \vec{R}^{0F} = \left|\vec{X}^F\right| \cdot \begin{Bmatrix} \sin\theta^F\cos\varphi^F; \\ \sin\theta^F\sin\varphi^F; \\ \cos\theta^F \end{Bmatrix}, \quad (4)$$

where $\vec{X}^F$ – radius vector of point F; $\left|\vec{X}^F\right|$ – vector length; $\vec{R}^{0F}$ – unit vector; φ^F, θ^F – azimuth and angle of point F, then it is necessary to provide phase of complex current amplitude in each radiator for sharp directional radiation of CPA in point with radius vector (4):

$$\arg(\dot{I}_{nm}) = -k_0\left(\vec{R}_n^{\,0F} \cdot \vec{X}^F + \left|\vec{X}^F - \vec{X}_n\right|\right). \quad (5)$$

More generally one designate the field of CPA radiation by way of fields superposition (1), (2):

$$\dot{\vec{E}}\left(\vec{X}\right) = \frac{k_0}{j4\pi}\sqrt{\frac{\mu_0}{\varepsilon_0}}\sum_{n=0}^{N-1}\frac{\dot{I}_n}{R_n}\vec{s}_n^{\,T} \cdot e^{jk_0\left(\vec{R}_n^{\,0}\vec{X}+R_n\right)}; \quad (6)$$

$$\dot{\vec{H}}(\vec{X}) = -\frac{k_0}{j4\pi}\sum_{n=0}^{N-1}\frac{\dot{I}_n}{R_n}\vec{s}_n^{\,\perp} \cdot e^{jk_0\left(\vec{R}_n^{\,0}\vec{X}+R_n\right)}, \quad (7)$$

where $\left|\dot{I}_n\right|$ – amplitude distribution of currents (3) in CPA which is symmetrical to direction main pattern.

One research analysis CPA DC for following cases:

– all CPA elements radiate. They all are allocated in free space, CPA field is designated expressions (6), (7);

– part of CPA elements radiate with coordinates $\varphi_n \in \phi_0$, allocated in bounds of circular excitation sector ϕ_0 (fig. 2) and create arc array (AA);

– AA elements radiate, allocated in bounds of excitation sector ϕ_0 above ideally conducting surface (CS) used in the shape of circular endless thin cylinder, radius and height is much bigger λ_0 - CS AA. Then one can consider that CS allocated near each dipole accordingly to principle of locality is locally plane. One should use method of mirror images for accounting influence of conducting surface on DC [3]. Boundary conditions on CS $\dot{E}^T(S) = 0$ will satisfy the expression for radiation field if dipoles above antenna surface will be on the height $h=0,25\lambda_0$:

$$\dot{E}\left(\vec{X}\right) = \frac{k_0\sqrt{\frac{\mu_0}{\varepsilon_0}}}{j4\pi}\sum_{n=0}^{N-1}\dot{I}_n \times \left(\frac{\vec{s}_n{}^T}{R_n}e^{jk_0\left(\vec{R}_n{}^0\vec{X}+R_n\right)} + \frac{\vec{s}_n{}^{T\prime}}{R_n{}'}e^{jk_0\left(\vec{R}_n{}^{0\prime}\vec{X}+R_n{}'+\pi\right)}\right) \quad (8)$$

$$\dot{H}(\vec{X}) = -\frac{k_0}{j4\pi}\sum_{n=0}^{N-1}\dot{I}_n \times \left(\frac{\vec{s}_n{}^{\perp}}{R_n}e^{jk_0\left(\vec{R}_n{}^0\vec{X}+R_n\right)} + \frac{\vec{s}_n{}^{\perp\prime}}{R_n{}'}e^{jk_0\left(\vec{R}_n{}^{0\prime}\vec{X}+R_n{}'+\pi\right)}\right). \quad (9)$$

where $\vec{s}_n{}^{T\prime}$, $\vec{s}_n{}^{\perp\prime}$ – vector components $\vec{s}_n{}'$, taken into consideration orientation and dipole length of mirror image; $R_n{}'$ – range to OP from dipole, which is mirror to n-dipole.

One propose that CPA elements not to be allocated in light region towards main maximum of radiation $\vec{R}^{0F}$ do not excite. Thus for cases AA and CS AA one admit that array element is placed in the region of excitement and radiate if angle α_n^F (fig. 2) between ort of outer normal to radiator $\vec{N}_n^0$ and ort $\vec{R}_n{}^{0F}$ satisfy conditions:

$$\alpha_n^F = \arccos\left(\vec{N}_n^0 \cdot \vec{R}_n{}^{0F}\right) \in (-0,5\phi_0; 0,5\phi_0). \quad (10)$$

Value of sector ϕ_0 can be matched with concrete task used by antenna system.

By analogy one take into consideration bounds of light region in CS AA towards observation point $\vec{X}$. It should be taken into account that radiator is allocated in “light region” when $\vec{X}_n \approx \vec{X}_n{}'$, if angle α_n (fig. 2) between $\vec{N}_n^0$ and $\vec{R}_n{}^0$ satisfy conditions:

$$\alpha_n = \arccos\left(\vec{N}_n^0 \cdot \vec{R}_n{}^0\right) \in (-0,5\pi; 0,5\pi). \quad (11)$$

Taking into account (10), (11) that bounds region excitement of AA are designated by function:

$$\Xi\left(\alpha_n^F\right) = \begin{cases} 1 \ , \ \left(\vec{N}_n^0 \cdot \vec{R}_n{}^{0F}\right) \ge \cos(\phi_0/2) \\ 0 \ , \ \left(\vec{N}_n^0 \cdot \vec{R}_n{}^{0F}\right) < \cos(\phi_0/2) \end{cases}. \quad (12)$$

In mind (10), (11) bounds of excitation “light region" AA above CS are designated as function:

$$\Xi\left(\alpha_n^F, \alpha_n\right) = \begin{cases} 1 \ , \ \Xi\left(\alpha_n^F\right) = 1 \cup \left(\vec{N}_n^0 \cdot \vec{R}_n{}^0\right) \ge 0, \\ 0 \ , \ \Xi\left(\alpha_n^F\right) = 0 \cup \left(\vec{N}_n^0 \cdot \vec{R}_n{}^0\right) < 0. \end{cases} \quad (13)$$

Taking into consideration (12) AA field will be designated as:

$$\dot{E}\left(\vec{X}\right) = \frac{k_0}{j4\pi}\sqrt{\frac{\mu_0}{\varepsilon_0}}\sum_{n=0}^{N-1}\Xi\left(\alpha_n^F\right)\frac{\dot{I}_n}{R_n}\vec{s}_n{}^T e^{jk_0\left(\vec{R}_n{}^0\vec{X}+R_n\right)} \quad (14)$$

$$\dot{H}(\vec{X}) = -\frac{k_0}{j4\pi}\sum_{n=0}^{N-1}\Xi\left(\alpha_n^F\right)\frac{\dot{I}_n}{R_n}\vec{s}_n{}^{\perp} e^{jk_0\left(\vec{R}_n{}^0\vec{X}+R_n\right)}. \quad (15)$$

Taking into account (13) field of AA above CS will be designated by expressions:

$$\dot{E}\left(\vec{X}\right) = \frac{k_0\sqrt{\frac{\mu_0}{\varepsilon_0}}}{j4\pi}\sum_{n=0}^{N-1}\Xi\left(\alpha_n^F, \alpha_n\right)\dot{I}_n \times \left(\frac{\vec{s}_n{}^T}{R_n}e^{jk_0\left(\vec{R}_n{}^0\vec{X}+R_n\right)} + \frac{\vec{s}_n{}^{T\prime}}{R_n{}'}e^{jk_0\left(\vec{R}_n{}^{0\prime}\vec{X}+R_n{}'+\pi\right)}\right) \quad (16)$$

$$\dot{H}(\vec{X}) = -\frac{k_0}{j4\pi}\sum_{n=0}^{N-1}\Xi\left(\alpha_n^F, \alpha_n\right)\dot{I}_n \times \left(\frac{\vec{s}_n{}^{\perp}}{R_n}e^{jk_0\left(\vec{R}_n{}^0\vec{X}+R_n\right)} + \frac{\vec{s}_n{}^{\perp\prime}}{R_n{}'}e^{jk_0\left(\vec{R}_n{}^{0\prime}\vec{X}+R_n{}'+\pi\right)}\right). \quad (17)$$

Vertical and horizontal field components CPA in OP have following view:

$$\dot{E}^v\left(\vec{X}\right) = \dot{E}\left(\vec{X}\right)\vec{q}^v, \dot{H}^v\left(\vec{X}\right) = \dot{H}\left(\vec{X}\right)\vec{q}^v;$$
$$\dot{E}^h\left(\vec{X}\right) = \dot{E}\left(\vec{X}\right)\vec{q}^h, \dot{H}^h\left(\vec{X}\right) = \dot{H}\left(\vec{X}\right)\vec{q}^h,$$

where $\vec{q}^v$, $\vec{q}^h$ – orthogonal orts which designate polarization field in TC.

One can designate directivity in direction of main maximum with expression on condition that active phased array (APA) setting along axis is separated. But array consisted of dipoles is oriented across the OZ axis [A8]:

$$D \approx D^{\varphi}D^{\theta} = 3\pi\left(\int_0^{2\pi}\Psi\left(\theta = \theta^F, \varphi\right)d\varphi\right)^{-1} \quad (18)$$

where D^{θ}=1,5 – КСД elementary dipole; D^{φ} – AA directivity in azimuth plane; $\Psi(\theta,\varphi) = \left|\dot{F}^v(\theta,\varphi)\right|^2 + \left|\dot{F}^h(\theta,\varphi)\right|^2$ – power pattern, $\dot{F}^{v(h)}(\theta,\varphi) = \frac{\dot{E}^{v(h)}(\theta,\varphi)}{\max\left(\dot{E}^{v(h)}(\theta,\varphi)\right)}$ normalized complex field pattern on vertical and horizontal polarization.

2. Influence analysis APA and array spacing on the CPA directional characteristic

Maximum directivity - D; power pattern width in zero level - $2\varphi_{0,5P}$; sides lobe level of field pattern: the first - SLL_1, maximum - SLL_{max}, and their average level SLL_{med}. All of this is used for influence analysis APA and spacing between elements in CPA far-field region on the main polarization.

In the capacity of output data there was chosen: wave length λ_0=0,23 м; CPA diameter - 2 m; array spacing in bounds: $d_n = (0,5 \div 1)\lambda_0$; vertical polarization of radiators; direction of pattern main maximum $\theta^F = \varphi^F = 0$; height of radiators allocation above ideally conducting surface $h = 0,25\lambda_0$; sector of excitation AA and AA above CS $\phi_0 = 180^0$; amplitude separations (AS) are relatively symmetrically to pattern maximum and shown on the fig. 3.

For circular array, AA and AA above CS on the fig. 4 it is represented results of directivity dependences calculations, normalized to general number of elements in array. On the fig. 4 it is obviously that the maximum directivity (normalized to number of elements in array) is provided for CS AA when radius of array is fixed and the smallest one is for AA. Directivity is monotonously decreased in increasing array spacing when amplitude distributions in CS AA are slowly fallen down to the edges of light region (№1 and №2 on the fig. 4). CS AA directivity is monotonously increased in increasing array spacing when separations are fallen down to the edges of light region very much (№3...12 on the fig. 4). At the same time there is such value as d_n / λ_0. When this value is achieved, further increasing d_n spacing not to bring to the essential growth of directivity (increase is not bigger 10% from maximum value).

For the most distribution in CS AA this value is in the bounds 0,6...0,7, besides it is provided normalized directivity 1,28...1,3. In cases CPA and AA the directivity dependence on array spacing has more difficult (explosive) character. For CA the biggest value of normalized directivity does not exceed value 1,15. It concerns for all examined cases. The largest changes of directivity in changing CA spacing are in slowly falling down up to the edges by two equivalent subarrays. When there is arrays (№1, №2 on the fig. 4). Besides it is observed maximum directivity increase on the interval of normalized spacing value 0,5...0,63. For array №3...№9 and №11, №12 (fig. 4) in increasing spacing, array directivity is fallen down monotonously.

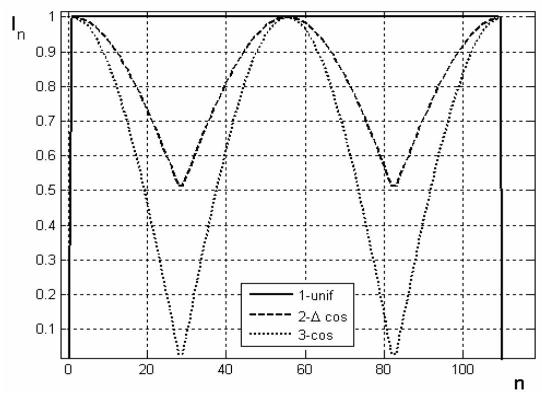

a: 1 – uniformly; 2 – cosine on the "pedestal" 0,5; 3 – cosine

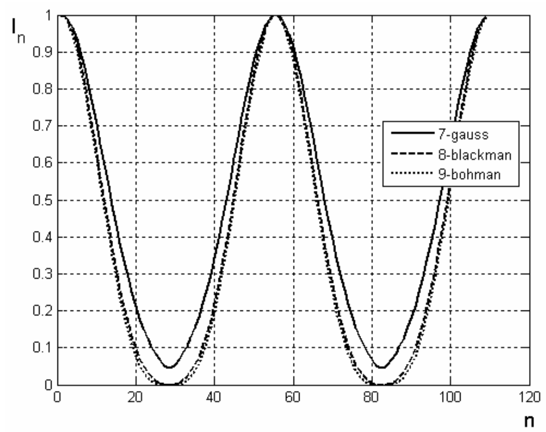

c: 7 – Gauss; 8 – Blackman; 9 – Bohman

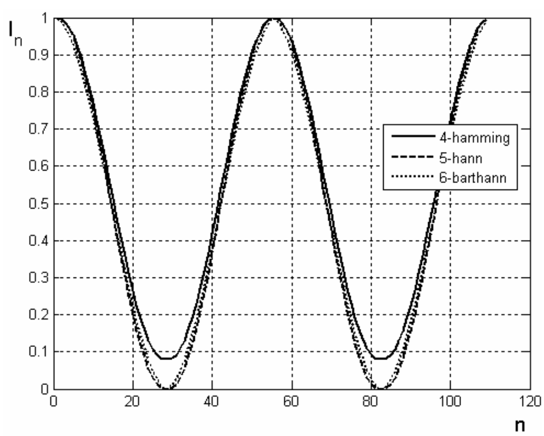

b: 4 – Hamming; 5 – Hana; 6 – Barthann

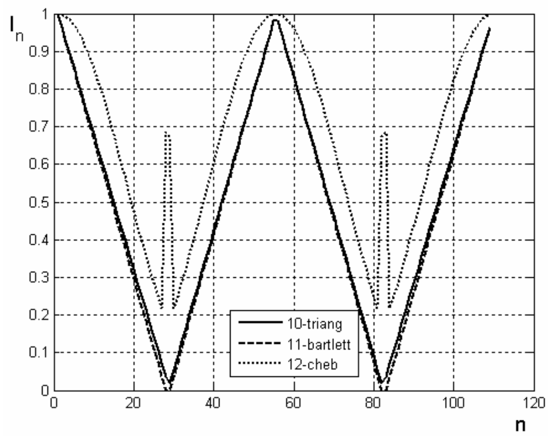

d: 10 – triangular; 11 – Barletta; 12 – Chebishev

Fig. 3. Amplitude distribution in CPA when $N = 108$

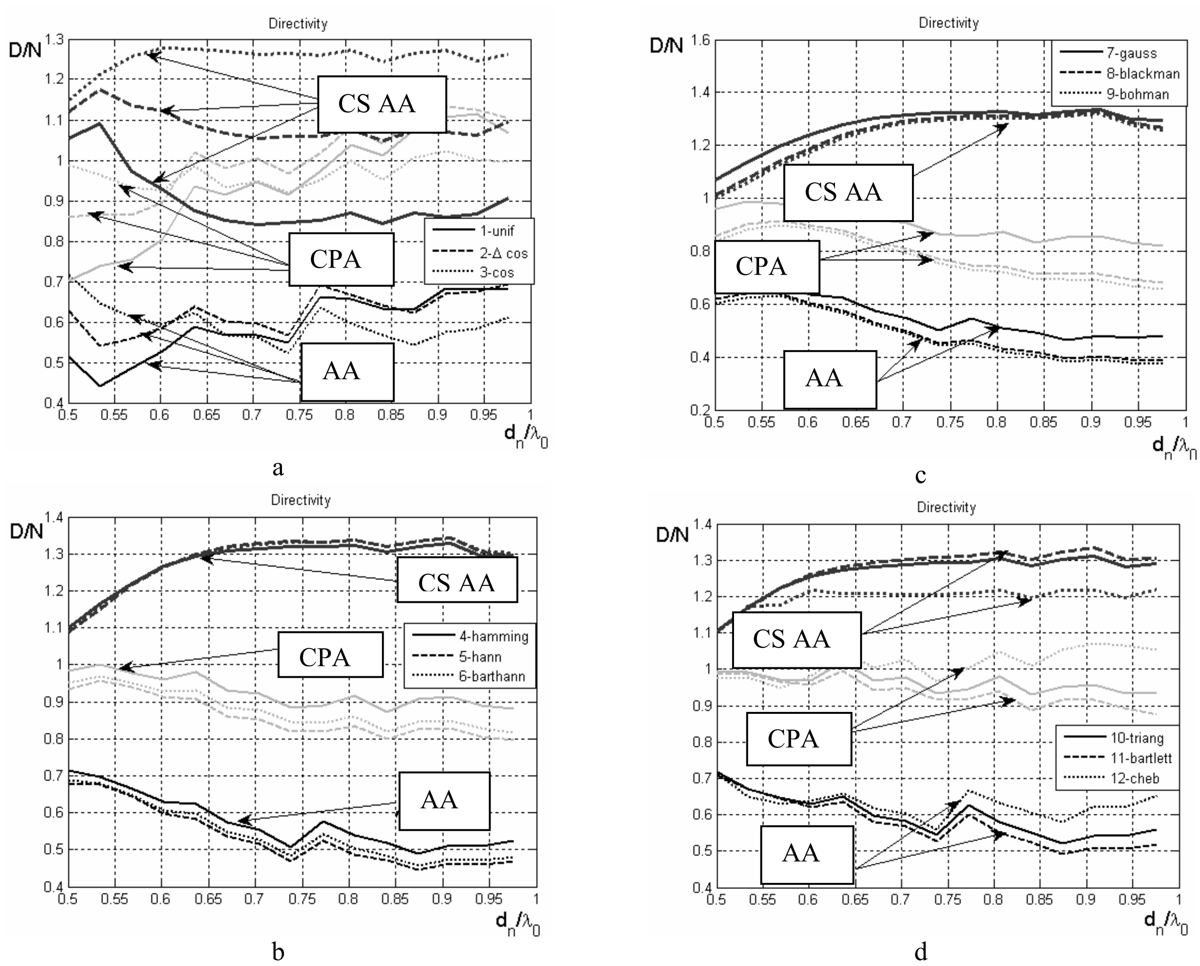

Fig. 4. Dependence of normalized directivity on array spacing

Absolute maximum of directivity is satisfied for normalized spacing 0,53...0,56 for arrays №3...№9 (fig. 4), and for value of normalized spacing 0,63...0,64 for arrays №11, №12 (fig. 4). At the same time the more amplitude is fallen down to the edges of subarrays the less directivity is changed together with array spacing (about 10% from maximum value for arrays №3...№11 on the fig. 4). For AA the most value of normalized directivity is not bigger than 0,72 in all examined cases. At whole the character of directivity dependences on array spacing coincide with CPA and AA.

On the fig. 5 there are dependences on array spacing the first side lobe level of directivity for different amplitude distribution. On the fig. 6 for different amplitude distribution it is displayed dependences of maximum lobes level in the directivity on spacing.

By results of analysis fig. 5, 6 one can make the following conclusions. In the case when radiators in array are allocated above CS it is provided the least side lobes level and maximum one for examined arrays.

For the row of array the first side lobe level in CS AA with array spacing is not changed (arrays №1…№3, №8, №9, №12 on the fig. 5) and it is -15…-12 dB. But for arrays №4…№7, №10 dependence the first side lobe level on array spacing has fluctuating character with row of extremums. Comparison of fig. 5 and fig. 6 display that for the most arrays in CS AA there is so boundary value of normalized array spacing for what the first side lobe level is maximum. So for arrays №1…№6 this bound of normalized array spacing lays in the bounds 0,6…0,64, and for arrays №8…№11 in bounds 0,53…0,54. Further increasing normalized array spacing brings to increasing far-out side lobes level and their angular width exceeds width of the main maximum pattern very much. For the most examined arrays, dependence the first side lobe level for CPA and AA on normalized array spacing is close to the monotonous one (fig. 5). At the same time when the normalized array spacing gets bigger that relative changes then the first side lobe level are insignificant (not bigger than 1 dB). The peculiarity of CPA and AA is exceeding the first side lobe level by far lobes in row of arrays (№4…№6, №10…№11 on the fig. 5 and on the fig. 6) by values of normalized spacing 0,5.

So for AA with separations of arrays №4…№6, №10…№11 the far-out side lobes level exceed the first side lobe level by 2,8…3,5 dB and 2,6…2,7 dB, accordingly. For arrays which are slowly fallen down to the edges of equivalent subarrays in CPA (№2 and №3 on the fig. 5), boundary value of normalized spacing in what the first side lobe level is stayed maximum and set on the level 0,57 for array №2 and 0,64 for array №3.

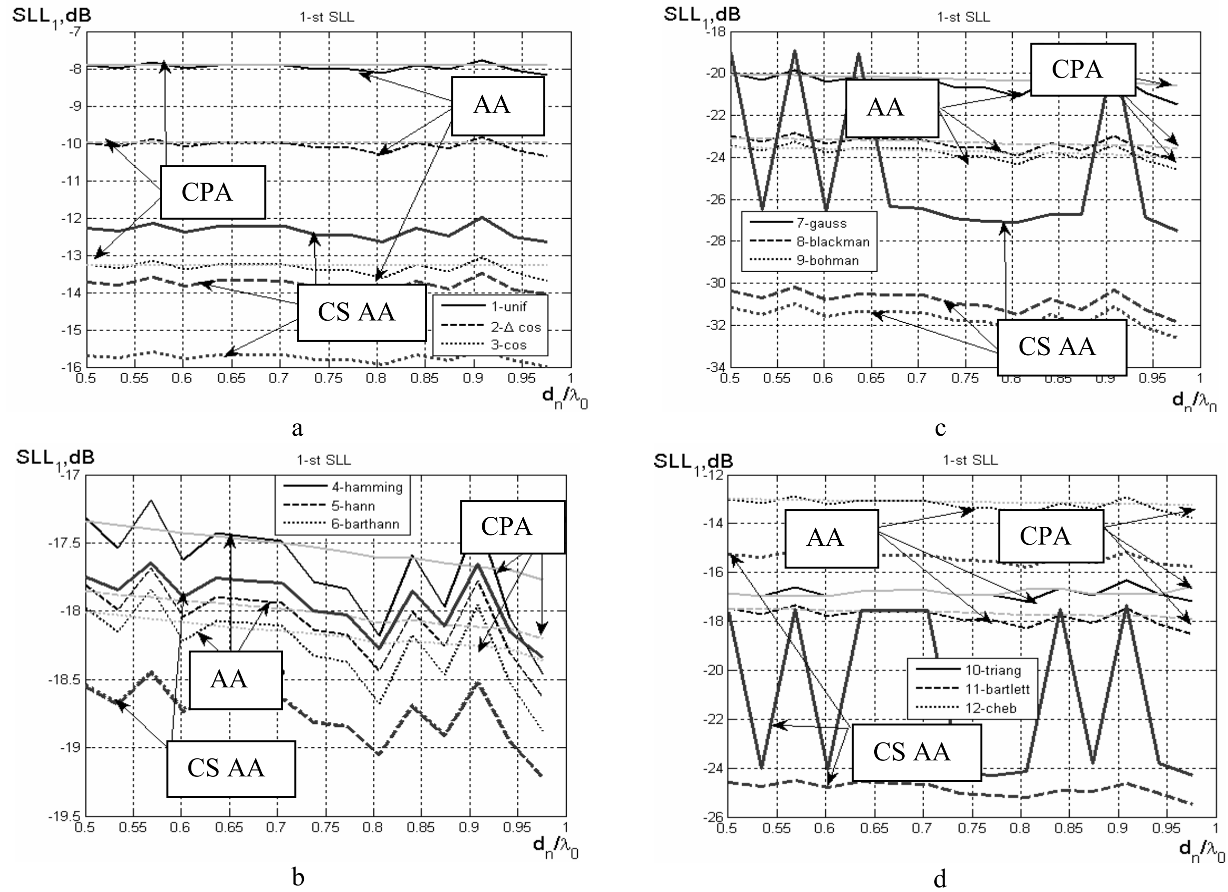

Fig. 5. Dependence the first side lobe level of pattern on array spacing

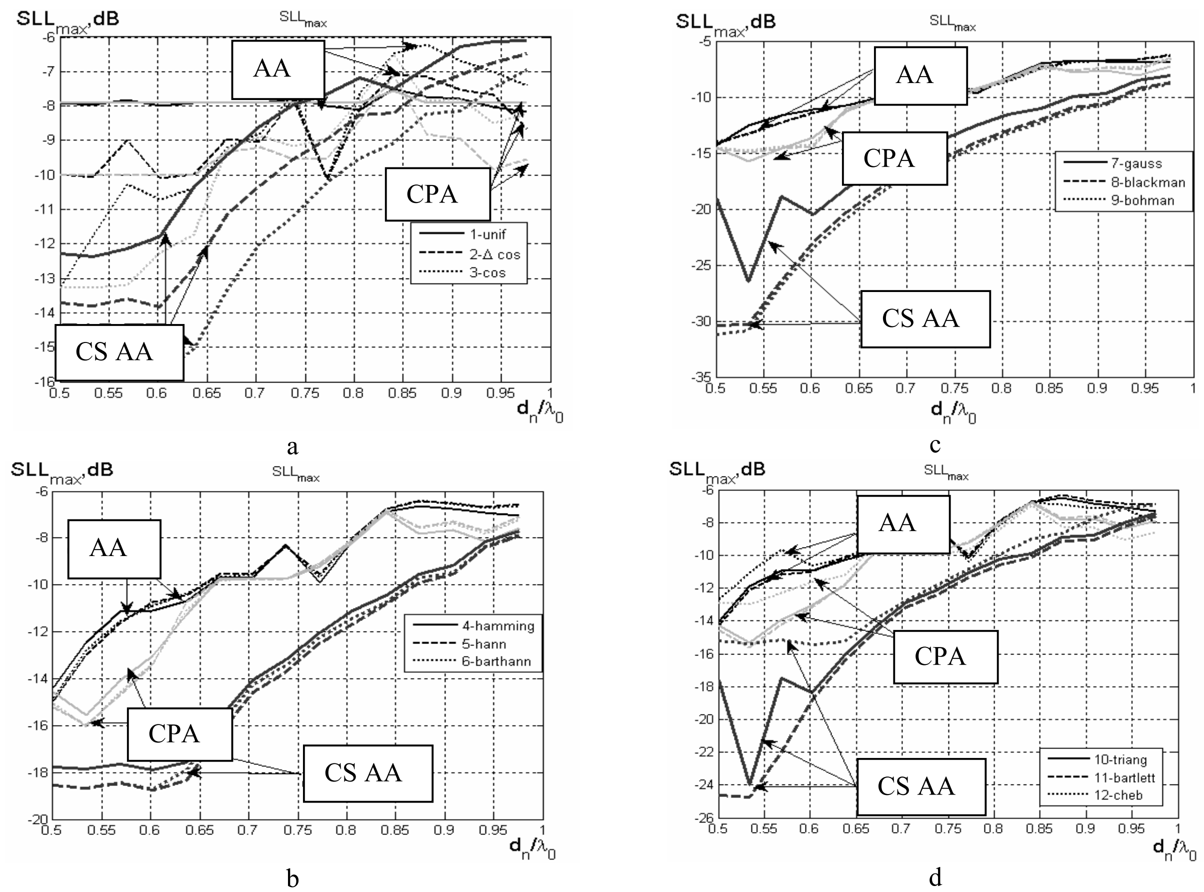

Fig. 6. Dependence the maximum side lobe level on array spacing

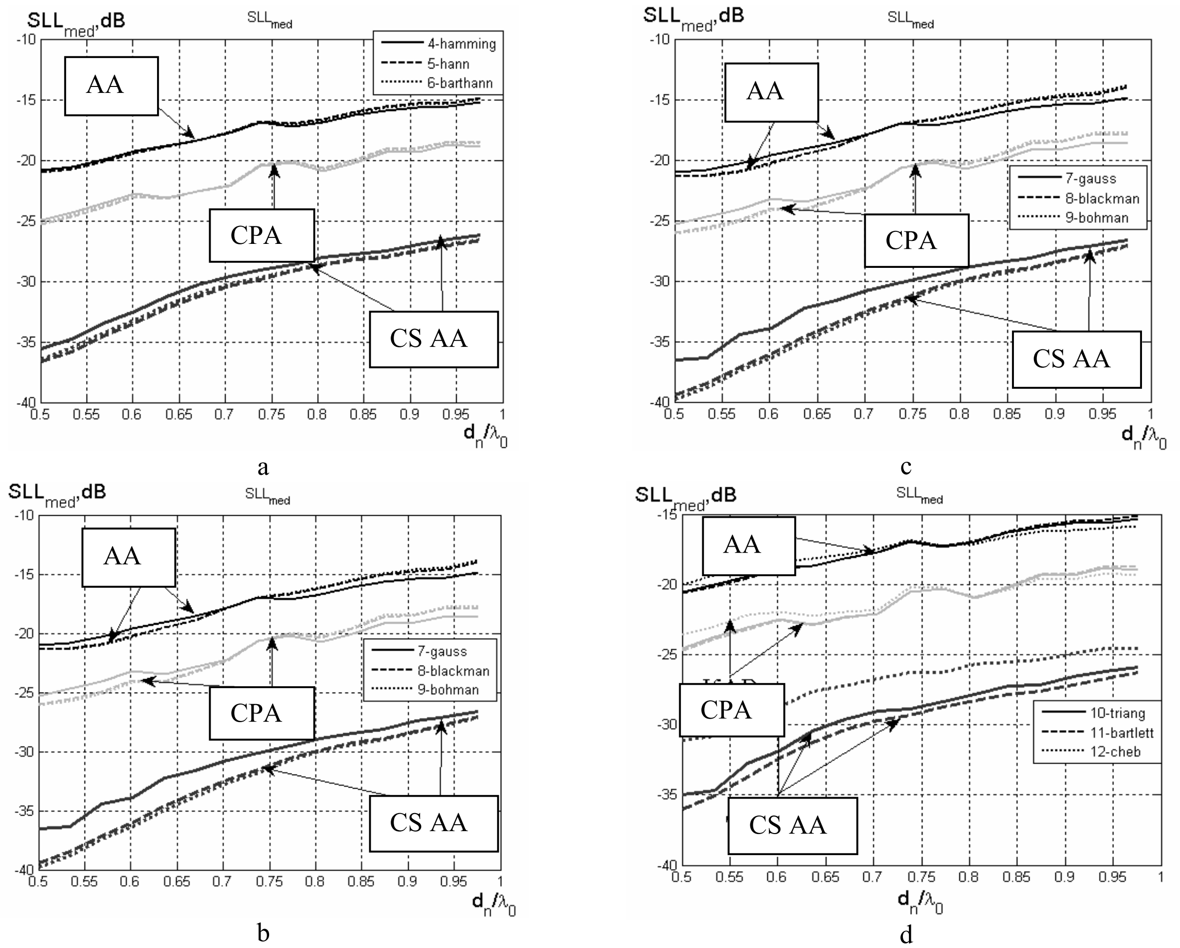

Fig. 7. Dependence average side lobe level of pattern on CPA spacing

When normalized spacing in CPA and AA is getting bigger then maximum side lobes are being approached to the main lobe.

On the fig. 7 it is displayed dependences average side lobe level on CPA spacing for different arrays. It seems that the least average side lobe level provides allocation of radiators above CS.

3. Recommendation for choosing CPA parameters and characteristics

Carried numerical analysis of array influence on directivity characteristics of CA displays that among examined radiating systems the best one is AA with allocation of elements above CS. CPA with allocated dipoles in free space have the worst characteristics. Examining all the variants one can make a conclusion that the best correlation directivity and side lobes level is provided when the value of a quantity of array spacing is set in bounds 0,55...0,7 λ_0 .

Further increasing value of array spacing excites increasing far-out side lobes CS AA and their moving to the main lobe of pattern.

In table 1 it is displayed directivity characteristics of CS AA and CPA for different arrays got for normalized array spacing 0,6 in quantity of radiators when N=92.

Table 1

Directivity characteristics of CPA for different amplitude distributions

Characteristics CS AA / CPA	№ Array					
	1	2	3	4	5	6
D / N	1,23 / 0,96	1,18 / 0,9	1,16 / 0,88	1,19 / 0,94	1,19 / 0,94	1,19 / 0,94
$2\varphi_{0,5P}^{deg\,ree}$	17,8 / 8,2	19,8 / 9,9	19,8 / 10,2	16,5 / 7,2	16,5 / 7,6	9,2 / 6,3
SLL_{max}^{-dB}	21,6 / 11,6	23,9 / 11,6	24,4 / 11,6	19,4 / 10,9	19,9 / 10,9	15,6 / 10,2
SLL_{1}^{-dB}	26,9 / 20,1	31,1 / 23,2	31,9 / 23,6	24,3 / 16,9	25 / 17,6	15,6 / 13,1
SLL_{med}^{-dB}	34,3 / 24,1	36,4 / 24,9	36,7 / 24,9	32,2 / 23,3	32,8 / 22,2	28,7 / 22,2
D / N	1,23 / 0,96	1,18 / 0,9	1,16 / 0,88	1,19 / 0,94	1,19 / 0,94	1,19 / 0,94
$2\varphi_{0,5P}^{deg\,ree}$	17,8 / 8,2	19,8 / 9,9	19,8 / 10,2	16,5 / 7,2	16,5 / 7,6	9,2 / 6,3
SLL_{max}^{-dB}	21,6 / 11,6	23,9 / 11,6	24,4 / 11,6	19,4 / 10,9	19,9 / 10,9	15,6 / 10,2
SLL_{1}^{-dB}	26,9 / 20,1	31,1 / 23,2	31,9 / 23,6	24,3 / 16,9	25 / 17,6	15,6 / 13,1
SLL_{med}^{-dB}	34,3 / 24,1	36,4 / 24,9	36,7 / 24,9	32,2 / 23,3	32,8 / 22,2	28,7 / 22,2

By results of influence analysis array type on side lobes levels it is set that there is a situation for arrays №4...№12 when far-out side lobes level exceed close side lobes level in some times. Besides directional characteristics of array in choosing variant of CA constructing one have to take into account quantity of array elements taken part in forming pattern. In general case field amplitude in far-field region is designated on the range R by expression [3]:

$$E \approx R^{-1}\sqrt{60P_{\Sigma} \cdot N \cdot C_D} \cdot \left|\dot{F}(\theta,\varphi)\right| \quad (19)$$

where P_{Σ} – total power of; $C_D = D/N$ – conversion factor between quantity of radiators and array directivity (table 1). If bounds excitation region of CS AA radiators coincide with "light" area, then upper mark of field intensity in target area has the following view:

$$E \approx R^{-1}\sqrt{60 \cdot 0,5N^2 \cdot P_n \cdot C_D{}^{CS.AA}}\left|\dot{F}(\theta,\varphi)\right|. \quad (20)$$

Each radiating element of CA has the following view:

$$E \approx R^{-1}\sqrt{60 \cdot N^2 \cdot P_n \cdot C_D{}^{CPA}}\left|\dot{F}(\theta,\varphi)\right|. \quad (21)$$

From (20) and (21) equations in comparison with allocation of radiators above CS one can see that the difference in CPA directivity in free space can be compensated for account for big quantity of elements which radiate (receive) signals. In the capacity of example on the fig. 8 it is displayed dependences of radiators quantity taken part in radiating (receiving) signals from normalized CPA.

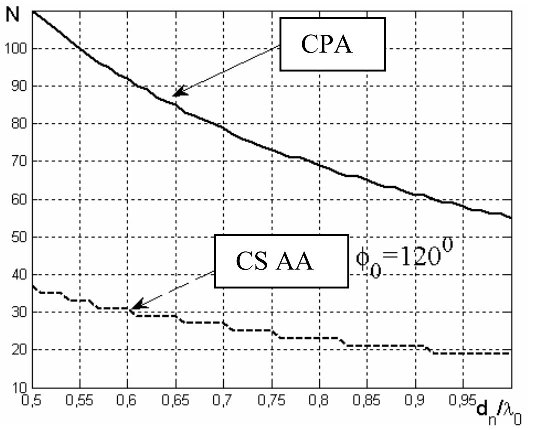

Fig. 8. Dependences of radiators quantity taken part in radiating (receiving) signals on normalized CPA

It should be noted that allocation of CPA radiators in free space can be more justified only after detailed accounting of diffraction effects, especially array interference.

Conclusions

By results of conducting analysis of CPA directional characteristics one can make the following conclusions:

– the main task in choosing type of amplitude distribution in CPA there is providing necessary the first and far-out side lobes level of pattern. Changing type of amplitude distribution in CPA and CS AA not to influence on changing directivity essentially (≤ 20%), but substantially influence on the width of main lobe (up to 200%) and side lobes level (up to -13 dB). The least side lobes are provided by Bohman amplitude distribution though it has the widest main lobe. Changing array spacing from 0,5 up to 0,7 λ_0 brings to increasing side lobes level from 2 dB to 3 dB depending on type of array;

– using CPA where radiators are allocated above conducting area there are only piece of radiators formed pattern. Relatively the main beam direction they are allocated in "light region". In this case the width of main beam is widened in comparison with CPA where radiators are allocated in free space. Side and far-out lobes level of pattern are decreased. in CS AA one can achieve side lobes level not better - 25 dB for account of changing array;

– using CPA where radiators are allocated in free space it is very difficult to achieve side lobes level less - 25 dB for account for changing only amplitude distribution. It is necessary to find the search of another methods for providing smaller side lobes level, for example in using concentric CPA;

– using CPA is necessary for establishing low-level radar field in radar system. In this antenna system, radiators are allocated above conducting surface.

References

1. Grib D.A. About possibilities of flexible control of radar field parameters in using in automatic low-level radar, circular active phased arrays and decimetric waves / D.A. Grib, V.O. Tutunik Data K NTC HUPS.– K.: HUPS, 2014.– P.193.

2. Method of mathematical modelling of directional characteristics axial-symmetric active arrays (for example of circular cylinder array of big electric sizes) / V.D. Karlov, I.G. Leonov, O.V. Lukashuk, A.F. Shevchenko // Armament system and defense technology. – 2008. – №1(13). – P. 97–102.

3. Antenna technology handbook: Handbook in 5 part. P. 1. By Y.N. Felda, E.G. Zelkina.- M.:IPRGR,1997.-256 p.

4. Josefsson L. Conformal array theory and design / L. Josefsson, P. Persson // New Jersey IEEE press. Whiley-Interscience publication, 2006, 488 p.

Надійшла до редколегії 20.02.2014

Рецензент: д-р техн. наук, проф. Ю.М. Седишев, Харківський університет Повітряних Сил ім. І. Кождеуба, Харків.

ПОРІВНЯЛЬНИЙ АНАЛІЗ ХАРАКТЕРИСТИК НАПРАВЛЕНОСТІ КІЛЬЦЕВИХ ФАЗОВАНИХ АНТЕННИХ РЕШІТОК ДЛЯ ЗАВДАНЬ СТВОРЕННЯ БАГАТОПОЗИЦІЙНИХ АКТИВНО-ПАСИВНИХ РЛС

М.М. Дергоусов, І.М. Трофимов, В.О. Тютюнник, А.Ф. Шевченко

Наведені результати чисельного аналізу залежностей характеристик спрямованості кільцевих антенних решіток утворених з елементарних електричних випромінювачів для різних видів амплітудно-фазових розподілів і значень конструктивних параметрів антенної системи. Результати можуть бути використані для вибору типу антен багатопозиційних активно-пасивних радіолокаційних систем призначених для створення суцільного радіолокаційного поля.

Ключові слова: *багатопозиційна активно-пасивна РЛС, кільцева фазована антенна решітка, характеристика спрямованості.*

СРАВНИТЕЛЬНЫЙ АНАЛИЗ ХАРАКТЕРИСТИК НАПРАВЛЕННОСТИ КОЛЬЦЕВЫХ ФАЗИРОВАННЫХ АНТЕННЫХ РЕШЕТОК ДЛЯ ЗАДАЧ СОЗДАНИЯ МНОГОПОЗИЦИОННЫХ АКТИВНО-ПАССИВНЫХ РЛС

М.М. Дергоусов, И.Н. Трофимов, В.А. Тютюнник, А.Ф. Шевченко

Приведены результаты численного анализа зависимостей характеристик направленности кольцевых антенных решеток, образованных из элементарных электрических излучателей для разных видов амплитудно-фазовых распределений и значений конструктивных параметров антенной системы. Результаты могут быть использованы для выбора типа антенн многопозиционных активно-пассивных радиолокационных систем, предназначенных для создания сплошного радиолокационного поля.

Ключевые слова: *многопозиционная активно-пассивная РЛС, кольцевая фазированная антенная решетка, характеристика направленности.*